

## Effect of Reynolds Number on Inclined Heated Semicircular Ducts at Different Rotations

E. A. El-Abeedy<sup>1</sup>, A. A. Busedra<sup>1</sup>

**Abstract:** Fully developed laminar mixed convection in inclined semicircular ducts is investigated numerically for the specific case of uniform heat input along the axial direction and uniform peripheral wall temperature, H1. The duct is considered over a variety of orientations (rotations) of its cross section, ranging from  $0^\circ$  (flat wall horizontally facing upward) to  $180^\circ$  (flat wall horizontally facing downward) with increment of  $45^\circ$  and a fixed inclination of its axis (with respect to the direction of gravity). In particular, the following conditions are considered: inclination  $\alpha = 20^\circ$ ,  $300 \leq Re \leq 1000$ ,  $Pr = 4$  and  $Gr = 1 \times 10^7$ . The combined effects induced by changes in the Reynolds number and duct orientation are presented in terms of the isovelcity and isotherm contours for the  $0^\circ$  and  $90^\circ$  cases (the flat wall in a vertical position). A decrease in the Reynolds number is shown to increase the heat transfer rate for all cross section orientations considered (more significant for the  $90^\circ$  orientation). The results also reveal a reduction in the friction factor when the  $90^\circ$  orientation is considered.

**Keywords:** Laminar Mixed Convection, Fully Developed, Semicircular Ducts.

### 1 Introduction

Due to the prominent importance of heat transfer in energy technology, several practical applications involving mixed convection in ducts of various cross sections continue to command substantial attention. The demand to produce more compact surfaces for heat exchangers and augment heat transfer, have led to the use of a variety of noncircular passages. The semicircular duct is an example of such noncircular passages typically used in compact heat exchangers. Heat transfer is strongly dependent on the geometry, inclination (up-flow and down-flow), and duct rotations (orientation of its cross section), as well as, the thermal boundary condition and fluid type. Therefore, mixed convection in inclined ducts of various cross sections has attracted much interest. A vast literature is available in the case of

---

<sup>1</sup> Department of Mechanical Engineering, University of Benghazi, Benghazi, Libya.

natural or mixed convection in classical geometries. As recent and relevant examples the reader may consider Abbassi, Halouani, Chesneau and Zeghmati (2011); Amirouche and Bessaïh (2012); Dihmani, Amraoui, Mezrhab and Laraqi, (2012); Ferahta, Bougoul, Médale and Abid, (2012); Kriaa, El Alami, Najam and Semma, (2011); Lappa (2004-2013); Meskini, Najam and El Alami, (2011); Rouijaa, El Alami, Semma and Najam, (2011). Efforts specifically devoted to semicircular ducts, however, seem to be relatively limited. Orfi and Galanis (1993) investigated the effect of tube inclination, as well as that of Grashof and Prandtl numbers on the laminar fully developed incompressible flow in uniformly heated tubes. The numerical method that employed to solve the problem is based on the SIMPLER method (Patanker (1980)). They found that for a given fluid and Grashof number there exists an optimum tube inclination, which maximizes the average Nusselt number. Busedra and Soliman (1999) studied the problem of laminar, fully developed mixed convection in inclined semicircular ducts ( $90^\circ$  orientation) under buoyancy assisted and buoyancy opposed conditions. Two thermal boundary conditions were used; H1 and H2 (uniform heat input axially with uniform wall heat flux circumferentially). The governing equations were solved numerically by using the finite control volume approach. They obtained results for the whole range of inclinations ( $-\pi/2 \leq \alpha \leq \pi/2$ ),  $Pr = 7$ , and wide range of  $Re$  and  $Gr$  ( $Gr$  up to  $2 \times 10^6$ ) friction factor and Nusselt number. They also reported that, for both H1 and H2 conditions and at a high  $Gr$ ; the Nusselt number develops a trend whereby its value increases with  $\alpha$  up to a maximum and then decreases with further increase in  $\alpha$ .

Other previous studies that dealt with mixed convection in horizontal semicircular ducts are those by Nandakumar, Masliyah and Law (1985). They studied the fully developed mixed convection with the H1 thermal boundary condition in a horizontal finless semicircular duct with the flat wall at the bottom. Lei and Trupp (1990) studied the same problem considered in Nandakumar, Masliyah and Law (1985) with the flat wall on top. Their results showed that, values of Nusselt number for the flat wall on top are approximately the same as for the flat wall at the bottom (Nandakumar, Masliyah and Law (1985)). Chinporoncharoenpong, Trupp and Soliman (1993) investigated the same problem by rotating the semicircular duct from  $0^\circ$  (the flat wall on top) to  $180^\circ$  (the flat wall at the bottom) with an incremental angle of  $45^\circ$ . They found that, orienting the flat wall of the semicircular duct vertically  $90^\circ$  up to  $135^\circ$  gave the highest heat transfer rate among the other orientations. Chinporoncharoenpong, Trupp and Soliman (1994) extended their study to horizontal circular sector ducts. Busedra and El-Abeedy (2003) studied the same problem considered in Chinporoncharoenpong, Trupp and Soliman (1993) by inclining the semicircular duct at a fixed angle and single value of Reynolds number.

They reported that, the effect of inclination is important in heat transfer enhancement, particularly when the flat wall of the duct is oriented at  $90^\circ$ . Busedra and Soliman (2000) studied the combined free and forced convection experimentally for laminar water flow ( $500 \leq Re \leq 1500$ ) in the entrance region of a semicircular duct,  $90^\circ$  oriented, with upward and downward inclinations within  $\pm 20^\circ$ . They concluded that for the upward inclinations,  $Nu$  increases with  $Gr$  and with  $\alpha$  (up to  $20^\circ$ ), while the effect of  $Re$  was found to be weak. Other numerical results for laminar flow in the entrance region were reported for horizontal semicircular ducts with the flat wall on top by El-Hasadi, Busedra and Rustum (2007) and for vertical semicircular ducts by Elsharif, Busedra and El-Hasadi (2009).

The duct rotation affects the cross-stream flow pattern and hence the heat transfer performances. The main objective of this paper is to investigate such effects for fully developed laminar mixed convection in semicircular ducts. Chinporoncharoenpong, Trupp and Soliman (1993) considered all the possible orientations (rotations) of the semicircular cross section but they limited to the horizontal case ( $\alpha = 0^\circ$ ) and without  $Re$  effects. Since Busedra and Soliman (1999) found that at high  $Gr$ , the Nusselt number attains a maximum value when  $\alpha = 20^\circ$ , here the problem is studied for such a value of  $\alpha$ . In particular, the effects of the cross section orientation (rotations) and  $Re$  on the velocity and temperature profiles, fluid flow and heat transfer rate are investigated assuming the H1 boundary condition and  $Gr = 1 \times 10^7$ .

## 2 Analysis and Modeling

The geometry under consideration is shown in Fig. 1 which represents a semicircular duct inclined at an angle of  $20^\circ$ . The duct is allowed to rotate to a desired orientation angle. The fluid is assumed to be incompressible and Newtonian, and the flow is steady, laminar, and fully developed hydrodynamically and thermally. Viscous dissipation and axial heat diffusion are assumed to be negligible. Fluid properties are assumed to be constant, except for the density variation in the buoyancy terms, which varies with temperature according to the Boussinesq approximation. Heat input is assumed to be uniform axially with uniform peripheral wall temperature.

For the considered three-dimensional flow problem, we will follow a parabolized Navier-Stokes procedure with the pressure approximation used in Anderson, Tannehill and Pletcher (1984). Thus, the pressure is expressed as:

$$p(r, \theta, z) = p_1(z) + p_2(r, \theta) \quad (1)$$

where  $p_1$  is the cross-sectional average pressure, which is assumed to vary linearly in the axial direction, while  $p_2$  provides the driving force for the secondary flow

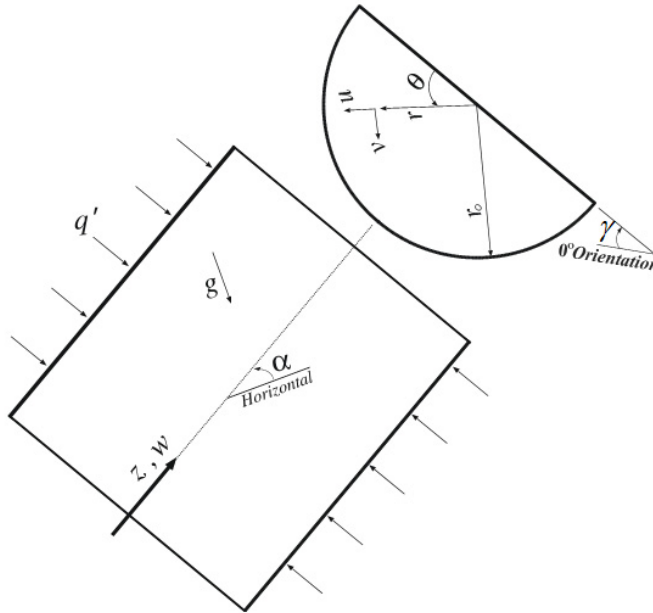


Figure 1: Geometry and coordinate system

within the cross section. With these considerations, the governing equations for the present problem are:

Continuity equation:

$$\frac{1}{R} \frac{\partial(RU)}{\partial R} + \frac{1}{R} \frac{\partial(V)}{\partial \theta} = 0 \quad (2)$$

Momentum equation:

R-direction:

$$U \frac{\partial U}{\partial R} + \frac{V}{R} \frac{\partial U}{\partial \theta} = -\frac{\partial P_2}{\partial R} + \nabla^2 U - \frac{2}{R^2} \frac{\partial V}{\partial \theta} - \frac{U}{R^2} + \frac{V^2}{R} - GrT \cos \alpha \sin(\theta - \gamma) \quad (3)$$

$\theta$ -direction:

$$U \frac{\partial V}{\partial R} + \frac{V}{R} \frac{\partial V}{\partial \theta} = -\frac{1}{R} \frac{\partial P_2}{\partial \theta} + \nabla^2 V + \frac{2}{R^2} \frac{\partial U}{\partial \theta} - \frac{V}{R^2} - \frac{UV}{R} - GrT \cos \alpha \cos(\theta - \gamma) \quad (4)$$

Z-direction:

$$U \frac{\partial W}{\partial R} + \frac{V}{R} \frac{\partial W}{\partial \theta} = -\frac{\partial P_1}{\partial Z} + \nabla^2 W + 2 \left( \frac{\pi}{\pi + 2} \right) \left( \frac{Gr}{Re} \right) T \sin \alpha \quad (5)$$

Energy Equation:

$$\text{Pr} \left( U \frac{\partial T}{\partial R} + \frac{V}{R} \frac{\partial T}{\partial \theta} \right) = \nabla^2 T - \left( \frac{2}{\pi} \right) W \quad (6)$$

The following equation (Eq.(7)) represents the dimensionless parameters and variables.

$$\begin{aligned} R &= \frac{r}{r_o}, \quad Z = \frac{z}{r_o}, \quad U = \frac{ur_o}{v}, \quad V = \frac{vr_o}{v}, \quad W = \frac{w}{w_m} \\ T &= \frac{t-t_w}{q'/k}, \quad P_1 = \frac{p_1^* r_o}{\rho v w_m}, \quad p_1^* = p_1 + \rho_w g z \sin \alpha \\ D_h &= \left( \frac{2\pi}{\pi+2} \right) r_o, \quad P_2 = \frac{p_2^* r_o^2}{\rho v^2}, \quad p_2^* = p_2 + \rho_w g r \cos \alpha \cos \theta \\ Re &= \frac{D_h w_m}{v}, \quad \text{Pr} = \frac{\rho v C_p}{k}, \quad Gr = \frac{g \beta q' r_o^3}{k v^2} \end{aligned} \quad (7)$$

The applicable boundary conditions are

$$U = V = W = 0 \quad (\text{on all walls}), \quad (8a)$$

$$T = 0 \quad (\text{on all walls}) \quad (8b)$$

Two important parameters used in engineering design are  $Nu$ , given by

$$Nu = \frac{h D_h}{k} = - \frac{2\pi}{(\pi+2)^2} \frac{1}{T_b} \quad (9)$$

$$\text{where, } T_b = \frac{2}{\pi} \int_0^{\pi} \int_0^1 W T R dR d\theta$$

and the friction factor  $f$  is defined by

$$f = \bar{\tau}_w / \frac{1}{2} \rho w_m^2 \quad (10)$$

The parameter  $\bar{\tau}_w$  was calculated by averaging the wall shear stress around the circumference of the semicircular duct. Thus:

$$f Re = \frac{4\pi}{(\pi+2)^2} \left[ \int_0^1 \left( \frac{\partial W}{R \partial \theta} \right)_{\theta=0} dR - \int_0^1 \left( \frac{\partial W}{R \partial \theta} \right)_{\theta=\pi} dR - \int_0^{\pi} \left( \frac{\partial W}{\partial R} \right)_{R=1} d\theta \right] \quad (11)$$

## 2.1 Solution Technique

The dimensionless governing partial differential equations, (Eqs (2)-(6)), were discretized by using a control volume based finite difference method (Patanker, 1980), and the power law scheme was used for the treatment of the convection and diffusion terms. The velocity-pressure coupling was handled using the SIMPLER algorithm. A staggered grid was used in the computations with uniform subdivisions in the  $R$  and  $\theta$  directions. The control volumes adjacent to the boundary were subdivided into two control volumes in order to capture the steep gradients in the temperature and axial velocity to insure obtaining accurate values of the wall shear stress. For given values of the input parameters  $Re$ ,  $Pr$ ,  $\alpha$ ,  $\gamma$ , and  $Gr$ , computations started with guessed field of  $U$ ,  $V$ ,  $W$ ,  $T$ , and  $fRe$ . The discretized equations were solved simultaneously for each radial line using the tridiagonal matrix algorithm [TDMA], and the domain was covered by sweeping line by line in the angular direction. The convergence is judged by the relative differences between the current and the previous iterative values of each primitive variable at each nodes being smaller than  $10^{-6}$ . The mass source terms which indicate local continuity of each control volume and the  $fRe$  correction which indicates overall axial mass balance are also required to be smaller than  $10^{-6}$ .

Verification of the present analysis was conducted for pure forced convection in order to determine the appropriate grid size. A sample of these results is shown in Tab. 1 for the forced convection case. The selected grid size of  $30 \times 75$  ( $R \times \theta$ ) is capable of producing  $Nu_o$  value of 4.0879 and  $fRe_o$  value of 15.7598 for pure forced convection. Comparing these results with the exact solutions of  $Nu_o = 4.089$  and  $fRe_o = 15.77$  in Sparrow and Haji-Sheikh (1966), it can be seen that the  $30 \times 75$  grid is sufficient to obtain accurate  $Nu$  and  $fRe$  values that are in excellent agreement with the exact values.

Table 1: Effect of grid size on  $Nu_o$  and  $fRe_o$  for  $Gr = 0$

| <i>Mish size</i> | $Nu_o$ | $fRe_o$ |
|------------------|--------|---------|
| 30 x 40          | 4.0896 | 15.7396 |
| 30 x 75          | 4.0879 | 15.7598 |
| 40 x 60          | 4.0914 | 15.7553 |
| 60 x 96          | 4.0996 | 15.7631 |

The accuracy of the present results for the inclined case ( $\alpha = 20^\circ$ ), over the rotation of  $90^\circ$  is also compared to data of Busedra and Soliman (1999), for  $Pr=7$ , and  $Re=500$  at  $Gr=1 \times 10^6$ . The approximate  $Nu$  value that extracted from graphical

results of (Busedra and Soliman 1999) is 12.27 which agree within 0.35% with the present value.

### 3 Results and Discussion

The inclined semicircular duct was considered over a variety of orientations of its cross section, ranging from  $0^\circ$  to  $180^\circ$  with increment of  $45^\circ$  and a fixed inclination of its axis. Numerical solutions are presented for H1 thermal boundary condition,  $Pr = 4$ ,  $\alpha = 20^\circ$ , different values of Reynolds number,  $300 \leq Re \leq 1000$ , and  $Gr = 1 \times 10^7$ . The whole range of duct orientations was covered to examine the overall quantity of  $Nu$ . The major results with  $Re = 500$  and wide range of  $Gr$  with the whole range of duct orientations have been reported by Busedra and El-Abeedy (2003). The effects of Reynolds number and duct orientation are presented in terms of the axial velocity and temperature distributions for  $\gamma = 0^\circ$  and  $90^\circ$  and three values of Reynolds number ( $Re = 300, 500, 1000$ ).

#### 3.1 Velocity Distribution

The axial velocity contours were plotted at equal intervals between the maximum and minimum, as shown in Figs. 2 and 3. The distortion of the velocity distribution increases with decreasing Reynolds number for both orientations. For the case of  $Re = 1000$ , the maximum velocity in Figs. 2-a and 3-a confines nearly to the center, while decreasing  $Re = 500$  shifts the velocity upward towards the upper part of the duct cross-section, as shown in Figs. 2-b and 3-b. At  $Re = 300$  the maximum axial velocity in Figs. 2-c and 3-c moves significantly towards the upper part of the duct. The location of the maximum velocity within the cross-section appears to be dependent on Reynolds number. It should be noted that, the buoyancy force is no longer acting normal to the main flow, since a component also exists in the flow direction. Thus only a component of the buoyancy force is driving the secondary flow due to the angle of inclination ( $\alpha = 20^\circ$ ). It can be seen that, the velocity increases in the upper part as Reynolds number decreases.

This is mainly due to the buoyancy term in the axial momentum equation (Eq.(5)), where the concentration of the velocity contours near the upper flat wall, Fig. 2-c, leads to increased wall shear stress. This amount of increase is clearly observed when the semicircular duct is oriented at  $0^\circ$ , as shown later. Further, the effect of  $Re$  plays a dominant rule in this phenomena. For  $Re = 1000$ , for example, a low velocity gradient can be noticed near the entire duct walls in both orientations, while, for  $Re = 300$ , a high velocity gradient appears near the entire flat surface of the  $0^\circ$  orientation and near the upper parts of the curved and flat walls of the  $90^\circ$  orientation.

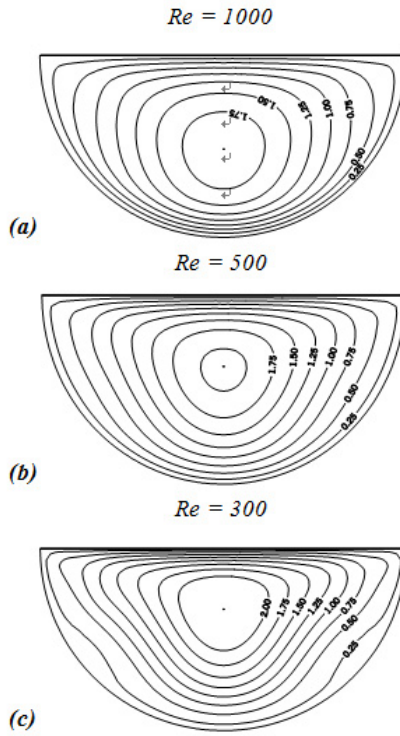


Figure 2: Velocity contours for 0° orientation

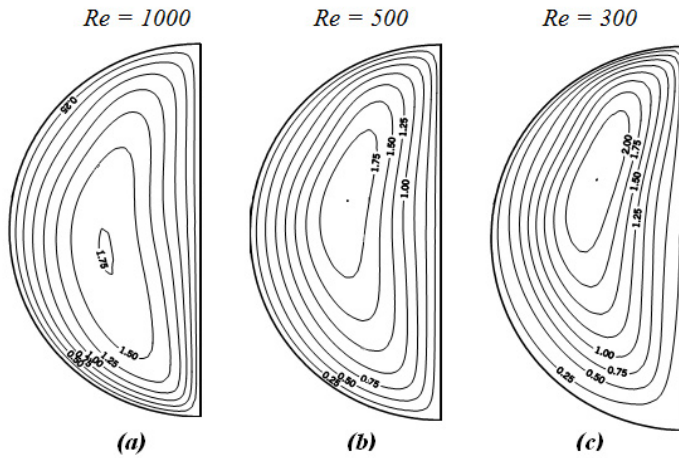


Figure 3: Velocity contours for 90° orientation

### 3.2 Temperature Distribution

The case of  $0^\circ$  orientation ( $\gamma = 0^\circ$ ) is illustrated in Fig. 4 to show the temperature distribution for  $Re = 300$ , 500, and 1000. All the distributions are symmetric and the minimum temperature, however, moves towards the lower part of the duct for all values of  $Re$ . The cooler fluid core decreases as  $Re$  decrease due to the increased intensity of the secondary flow. Consequently the enhancement in  $Nu$  is expected to increase due to free convection.

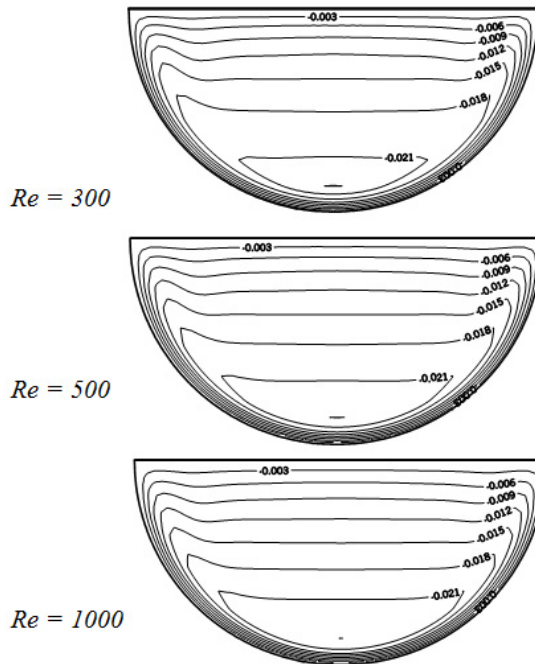


Figure 4: Temperature contours for  $0^\circ$  orientation

Fig. 5 shows the temperature distributions for  $\gamma = 90^\circ$  with the three values of Reynolds number. All the distributions are non-symmetric and the minimum temperature is still confined to the lower corner of the duct cross-section for all values of  $Re$ . The enhancement in  $Nu$  is expected to be much more pronounced for this orientation than for the case of  $0^\circ$  orientation. This is because of the corresponding secondary flow is stronger than that for  $\gamma = 0^\circ$ . Further, at low Reynolds number (*e.g.*;  $Re = 300$ ) the secondary flow is more intense than that for the cases of  $Re = 500$  and 1000. Thus  $Nu$  is expected to be higher for  $Re = 300$  than for  $Re = 500$  and 1000.

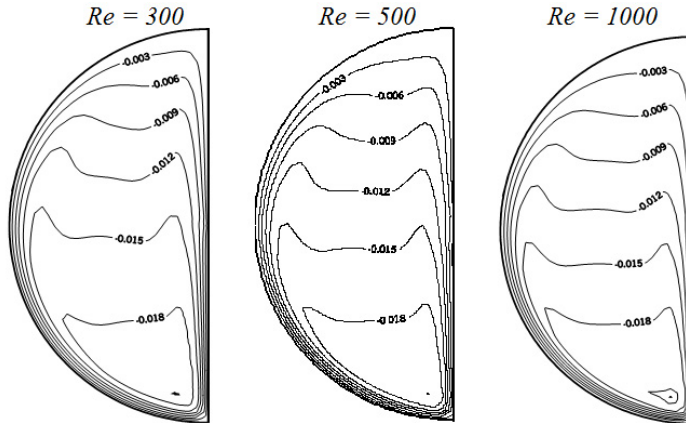


Figure 5: Temperature contours for  $90^\circ$  orientation

### 3.3 Nusselt Number and Friction Factor

Fig. 6 represents  $Nu/Nu_o$  with  $Re = 300, 500,$  and  $1000$  over a complete round of rotation from  $0^\circ$  to  $180^\circ$ . For  $Re = 300$ ,  $Nu$  values are the highest among all orientations. As  $Re$  increase to  $1000$ ,  $Nu$  values decrease due to the decrease of the buoyancy force. At  $\gamma = 0^\circ$ ,  $Nu/Nu_o$  decreased by  $3.2\%$  as  $Re$  increased from  $300$  to  $500$  and further decreased by  $6.4\%$  as  $Re$  increased from  $300$  to  $1000$ . Similarly for  $\gamma = 90^\circ$  the decrease of  $Nu/Nu_o$  values are  $1.8\%$  and  $4\%$ . It can be seen that,  $Nu/Nu_o$  values for  $\gamma = 0^\circ$  and  $180^\circ$  are almost the same. This is consistent with Lei and Trupp (1990) and Chinporoncharoenpong, Trupp and Soliman (1993).

Comparing the results of  $Nu$  for  $\gamma = 90^\circ$  with  $\gamma = 0^\circ$  are presented in Fig. 7. The results of  $Nu$ , for both rotations, decrease by increasing  $Re$ . This is due to the decreased intensity of the secondary flow. The trend of reduction in  $Nu$  is similar for both rotations. However, the values of  $Nu$  were always higher by  $15\%$  for  $\gamma = 90^\circ$  than that for  $\gamma = 0^\circ$ . In Fig. 8, the values of  $fRe$  are plotted against the rotations  $\gamma = 0^\circ$  and  $\gamma = 90^\circ$  with various values of  $Re$ . It can be seen that,  $fRe$  values at  $\gamma = 0^\circ$  are the highest for all values of  $Re$ . As the semicircular started to rotate from  $\gamma = 0^\circ$  towards  $90^\circ$ ,  $fRe$  values decrease. At  $Re = 300$ ,  $fRe$  values are the highest among those of  $Re = 500$  to  $1000$  for both orientations.

At  $\gamma = 0^\circ$ ,  $fRe$  decreased by  $15\%$  as  $Re$  increased from  $300$  to  $500$  and further decreased by  $24\%$  as  $Re$  increased from  $300$  to  $1000$ . Similarly, for  $\gamma = 90^\circ$ , the decrease in  $fRe$  values are  $7\%$  and  $9\%$ . However, for the case of  $90^\circ$ , increasing  $Re$  from  $500$  to  $1000$  gives a reduction in  $fRe$  by only  $2\%$  indicating that  $Re \geq 500$  has a small effect on  $fRe$  which is consistent with Busedra and Soliman (2000).

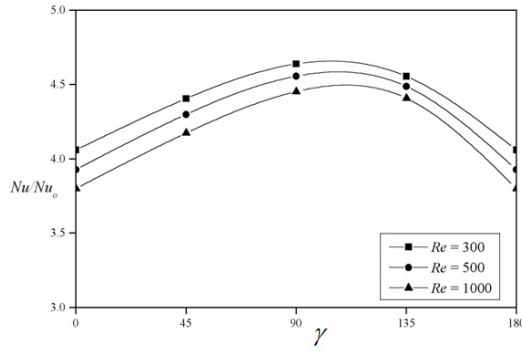


Figure 6: Effect of  $Re$  on  $Nu$  for all rotations

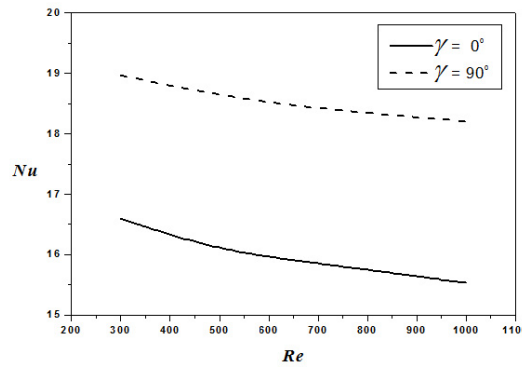


Figure 7: Effect of  $Re$  on  $Nu$  for  $\gamma = 0^\circ$  and  $\gamma = 90^\circ$

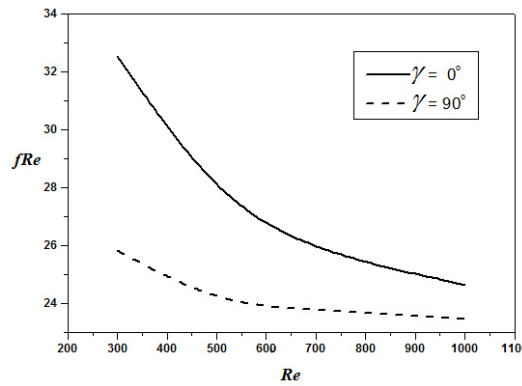


Figure 8: Effect of  $Re$  on  $fRe$  for  $\gamma = 0^\circ$  and  $\gamma = 90^\circ$

#### 4 Conclusions

The problem involving fully developed laminar mixed convection in semicircular ducts inclined at  $20^\circ$  with the H1 thermal boundary condition has been numerically investigated. Results have led to the following conclusions:

Regardless of the considered cross section orientation, the heat transfer rate can be enhanced by inclining the duct upward and assuming an inclination angle of  $20^\circ$ . However,  $Nu$  values for the symmetric orientation ( $\gamma = 0^\circ$ ) are lower than those for non-symmetric orientations ( $\gamma = 90^\circ$ ). On the other hand,  $fRe$  values are higher for  $\gamma = 0^\circ$  than for  $\gamma = 90^\circ$ .

For a complete round of rotation with  $45^\circ$  increments starting from  $0^\circ$  up to  $180^\circ$ , the highest  $Nu$  value occurs at a rotation angle of  $90^\circ$  associated with lowest  $fRe$  value. Thus, it is argued that, the  $90^\circ$  orientation can be seen at the same time as the higher limit for the heat transfer enhancement and the lower limit for the friction factor, while the  $0^\circ$  orientation represents the lower limit for the heat transfer rate and the higher limit for the friction factor.

#### References

- Abbassi, M.A.; Halouani, K.; Chesneau, X.; Zeghmami, B.** (2011): Combined Thermal Radiation and Laminar Mixed Convection in a Square Open Enclosure with Inlet and Outlet Ports. *Fluid Dyn. Mater. Process*, vol. 7, no. 1, pp. 71-96.
- Amirouche, Y.; Bessaïh, R.** (2012): Three-Dimensional Numerical Simulation of Air Cooling of Electronic Components in a Vertical Channel. *Fluid Dyn. Mater. Process*, vol. 8, no. 3, pp. 295-310.
- Anderson, D. A.; Tannehill, J. C.; Pletcher R. H.** (1984): Computational Fluid Mechanics and Heat Transfer. *McGraw-Hill, New York*.
- Busedra, A. A.; Soliman, H. M.** (1999): Analysis of Laminar Mixed Convection in Inclined Semicircular Ducts Under Buoyancy Assisted and Opposed Conditions. *Num. Heat Transfer, Part A*, vol. 36, pp. 527-544.
- Busedra, A. A.; El-abeedy, E. A.** (2003): Effect of Orientation on Laminar Mixed Convection for Inclined Semicircular Ducts, *Proc. 3<sup>rd</sup> Int. Conf. for Energy and Environment, Brack, Libya*.
- Busedra, A. A.; Soliman, H. M.** (2000): Experimental Investigation of Laminar Mixed Convection in an Inclined Semicircular Duct Under Buoyancy Assisted and Opposed Conditions. *Int. J. Heat Mass Transfer*, vol. 43, pp. 1103-1111.
- Chinporncharoenpong, C.; Trupp, A. C.; Soliman, H. M.** (1993): Effect of Gravitational force Orientation on Laminar Mixed Convection for a Horizontal Semicircular Duct. *Proc. 3<sup>rd</sup> World Conf. On Experimental Heat Transfer, Fluid*

*Mechanics and Thermodynamics*, vol. 109, pp. 131-137.

**Chinporncharoenpong, C.; Trupp, A. C.; Soliman, H. M.** (1994): Laminar Mixed Convection in Horizontal Circular Sector Duct. *Proc.10<sup>th</sup> International Heat Transfer Conf.*, vol. 5, pp. 447-452.

**Dihmani, N.; Amraqui, S.; Mezrhab, A.; Laraqi, N.** (2012): Numerical Modelling of Rib Width and Surface Radiation Effect on Natural Convection in a Vertical Vented and Divided Channel. *Fluid Dyn. Mater. Process*, vol. 8, no. 3, pp. 311-322

**El-Hasadi, Y. M. F.; Busedra, A. A.; Rustum, I. M.** (2007): Laminar Mixed Convection in the Entrance Region of Horizontal Semicircular Ducts with the Flat wall on Top. *ASME J Heat Transfer*, vol. 129, pp. 1203-1211.

**Elsharif, N. A.; Busedra, A. A.; El-Hasadi, Y.** (2008): Development of Laminar Mixed Convection in Vertical Semicircular Ducts. *Proc. Int. Symposium on Advances in Computational Heat Transfer CHT-08*, Marrakech, Morocco.

**Ferahta, F.Z.; Bougoul, S.; Médale, M.; Abid, C.,** (2012), Influence of the Air Gap Layer Thickness on Heat Transfer Between the Glass Cover and the Absorber of a Solar Collector. *Fluid Dyn. Mater. Process*, vol. 8, no. 3, pp. 323-338.

**Kriaa, M.; El Alami, M.; Najam, M.; Semma, E.** (2011): Improving the Efficiency of Wind Power System by Using Natural Convection Flows. *Fluid Dyn. Mater. Process*, vol. 7, no. 2, pp. 125-140.

**Lappa, M.** (2004): Combined effect of volume and gravity on the three-dimensional flow instability in non-cylindrical floating zones heated by an equatorial ring. *Physics of Fluids*, vol. 16, no. 2, pp. 331-343.

**Lappa, M.; Piccolo, C.; Carotenuto, L.** (2004): Mixed buoyant-Marangoni convection due to dissolution of a droplet in a liquid-liquid system with miscibility gap. *European Journal of Mechanics/B Fluids*, vol. 23, no.5, pp 781-794.

**Lappa, M.** (2005): Thermal convection and related instabilities in models of crystal growth from the melt on earth and in microgravity: Past history and current status. *Cryst. Res. Technol*, vol. 40, no. 6, pp. 531-549.

**Lappa, M.** (2007a): Secondary and oscillatory gravitational instabilities in canonical three-dimensional models of crystal growth from the melt, Part2: Lateral heating and the Hadley circulation. *Comptes Rendus Mécanique*, vol. 335, no (5-6) , pp. 261-268.

**Lappa, M.** (2007b): Secondary and oscillatory gravitational instabilities in canonical three-dimensional models of crystal growth from the melt, Part1: Rayleigh-Bénard systems. *Comptes Rendus Mécanique*, vol. 335, no. (5-6) , pp. 253-260.

**Lappa, M.** (2011): Some considerations about the symmetry and evolution of

chaotic Rayleigh–Bénard convection: The flywheel mechanism and the “wind” of turbulence. *Comptes Rendus Mécanique*, vol. 339, pp. 563–572.

**Lei, Q.; Trupp, A. C.** (1990): Predictions of Laminar Mixed Convection in a Horizontal Semicircular Duct. *6<sup>th</sup> Miami Int. Symposium on Heat and Mass Transfer*, vol. 4, pp. 10-12.

**Lappa, M.** (2013): On the Existence and Multiplicity of One-dimensional Solid Particle Attractors in Time-dependent Rayleigh–Bénard Convection. *Chaos*, vol. 23, no. 1, 013105.

**Meskini, A.; Najam, M.; El Alami, M.**(2011): Convective Mixed Heat Transfer in a Square Cavity with Heated Rectangular Blocks and Submitted to a Vertical Forced Flow. *Fluid Dyn. Mater. Process*, vol. 7, no. 1, pp. 97-110.

**Nandakumar, K.; Masliyah, J. H.; Law, H. S.** (1985): Bifurcation in Steady Laminar Mixed Convection Flow in Horizontal Ducts. *J. Fluid Mech.*, vol. 152, pp. 145-161.

**Rouijaa, H.; El Alami, M.; El Alami, Semma; Najam, M.** (2011): Natural Convection in an Inclined T-Shaped Cavity. *Fluid Dyn. Mater. Process*, vol. 7, no. 1, pp. 57-70.

**Orfi, J.; Galanis, N.** (1993): Laminar Fully Developed Incompressible Flow With Mixed Convection in Inclined Tube, *International Journal of Numerical Methods in Heat and Fluid Flow*, vol. 3, pp. 341-355.

**Patanker, S. V.** (1980): Numerical Heat Transfer and Fluid Flow, *Mc-Graw-Hill, New York*.

**Patanker, S. V.; Spalding, D. B.** (1972): A Calculation Procedure for Heat, Mass and Momentum Transfer in Three-Dimensional Parabolic Flows, *Int. J. Heat and Mass Transfer*, vol. 15, pp. 1787-1806.

**Sparrow, E.M.; Haji-Sheikh, A.** (1966): Flow and Heat Transfer in Ducts of Arbitrary Shape With Arbitrary Thermal Boundary Conditions, *J. Heat Transfer*, vol. 88, pp. 351-385.

## Nomenclature

|       |   |
|-------|---|
| $C_p$ | specific heat, J / kg k                               |
| $D_h$ | hydraulic diameter of the semicircular duct, m        |
| $f$   | friction factor                                       |
| $g$   | gravitational acceleration, m/s <sup>2</sup>          |
| $Gr$  | Grashof number  |
| $h$   | average heat transfer coefficient, W/m <sup>2</sup> k |
| $k$   | thermal conductivity of the fluid, W/m k              |

|       |  |
|-------|--|
| $Nu$  | average Nusselt number                         |
| $P$   | Pressure $N/m^2$                               |
| $p_1$ | cross- sectional average pressure, $N/m^2$     |
| $p_2$ | cross sectional excess pressure, $N/m^2$       |
| $P_1$ | dimensionless cross-sectional average pressure |
| $P_2$ | dimensionless cross-sectional excess pressure  |
| $Pr$  | Prandtl number                                 |
| $q'$  | rate of heat input per unit length, $W/m$      |
| $r$   | radial coordinate, $m$                         |
| $r_o$ | radius of circular wall, $m$                   |
| $R$   | dimensionless radial coordinate                |
| $Re$  | Reynolds number                                |
| $t$   | temperature, $K$                               |
| $T$   | dimensionless temperature                      |
| $u$   | radial velocity, $m/s$                         |
| $U$   | dimensionless radial velocity                  |
| $v$   | angular velocity, $m/s$                        |
| $V$   | dimensionless angular velocity                 |
| $w$   | axial velocity, $m/s$                          |
| $W$   | dimensionless axial velocity                   |
| $z$   | axial coordinate, $m$                          |
| $Z$   | dimensionless axial coordinate                 |

### *Greek Symbols*

|          |  |
|----------|--|
| $\alpha$ | inclination angle                          |
| $\beta$  | coefficient of thermal expansion, $k^{-1}$ |
| $\gamma$ | orientation angle                          |
| $\theta$ | angular coordinate, radians                |
| $\nu$    | kinematic viscosity, $m^2/s$               |
| $\rho$   | Density of the fluid, $kg/m^3$             |

### *Subscripts*

|   |                           |
|---|---------------------------|
| b | bulk value                |
| m | mean value                |
| o | corresponding to $Gr = 0$ |
| w | at the wall               |

